The Astrophysical Journal, 663:1103–1109, 2007 July 10

MASS AND TEMPERATURE OF THE TWA 7 DEBRIS DISK

Brenda C. Matthews
Herzberg Institute of Astrophysics, National Research Council of Canada, Victoria, BC V9E 2E7, Canada; brenda.matthews@nrc-cnrc.gc.ca

Paul G. Kalas
Department of Astronomy, University of California, Berkeley, CA 94720-3411; kalas@astron.berkeley.edu

and

Mark C. Wyatt
Institute of Astronomy, University of Cambridge, Cambridge CB3 0HA, UK; wyatt@ast.cam.ac.uk
Received 2007 January 2; accepted 2007 April 2

ABSTRACT

We present photometric detections of dust emission at 850 and 450 μm around the pre-main-sequence M1 dwarf TWA 7 using the SCUBA camera on the James Clerk Maxwell Telescope. These data confirm the presence of a cold dust disk around TWA 7, a member of the TW Hydrae Association (TWA). Based on the 850 μm flux, we estimate the mass of the disk to be 18 $M_{\rm lunar}$ (0.2 $M_{\oplus}$) assuming a mass opacity of 1.7 cm^2 g^{-1} with a temperature of 45 K. This makes the TWA 7 disk ($d = 55$ pc) an order of magnitude more massive than the disk reported around AU Microscopii (GL 803), the closest (9.9 pc) debris disk detected around an M dwarf. This is consistent with TWA 7 being slightly younger than AU Mic. We find that the mid-IR and submillimeter data require the disk to be comprised of dust at a range of temperatures. A model in which the dust is at a single radius from the star, with a range of temperatures according to grain size, is as effective at fitting the emission spectrum as a model in which the dust is of uniform size, but has a range of temperatures according to distance. We discuss this disk in the context of known disks in the TWA and around low-mass stars; a comparison of masses of disks in the TWA reveals no trend in mass or evolutionary state (gas-rich vs. debris) as a function of spectral type.

Subject headings: circumstellar matter — stars: individual (TWA 7) — stars: pre–main-sequence — submillimeter

1. INTRODUCTION

TWA 7 (2MASS J10423011−3340162, TWA 7A) is a weak-line T Tauri star identified as part of the TW Hydrae Association (TWA; Kastner et al. 1997) by Webb et al. (1999) based on the proper-motion studies in conjunction with youth indicators such as high lithium abundance, X-ray activity, and evidence of strong chromospheric activity. Disk systems were inferred around four of the 18 association members (Zuckerman & Song 2004) from measurements of IR excess with the *Infrared Astronomical Satellite* (*IRAS*). TW Hydra itself (a K7 pre-main-sequence star) hosts the nearest protostellar disk to the Sun. Another accreting disk is observed around one member of the triple system Hen 3-600 (Muzerolle et al. 2000), and two debris disk systems have been detected, around the A0 star HR 4796A (Jura 1991; Schneider et al. 1999) and one of two spectroscopic binary components of the quadruple system HD 98800 (Jayawardhana et al. 1999; Gehrz et al. 1999), which is a K5 dwarf. TWA 7 was not detected by *IRAS*.

Based on the width of the Li λ6707 line, Neuhäuser et al. (2000) deduced that TWA 7 is a pre-main-sequence star. TWA 7 was not detected by *Hipparcos*, but its membership in the TWA sets its distance to be 55 ± 16 pc (Neuhäuser et al. 2000; Weinberger et al. 2004; Low et al. 2005). Its spectral type is M1 based on LRIS (Low Resolution Imaging Spectrograph) spectra (Webb et al. 1999). Based on existing photometry, evolutionary tracks, and isochrone fitting, Neuhäuser et al. (2000) derived an age of 1–6 Myr (i.e., roughly coeval with other TWA stars) and a mass of 0.55 ± 0.15 $M_{\odot}$. The age of the association is generally taken to be ~8–10 Myr (Stauffer et al. 1995; Zuckerman & Song 2004). This is the age when planet formation is thought to be ongoing and when disk dissipation is occurring. Thus, the TWA is the ideal cluster in which to observe the transitions from pre-main-sequence stars with protoplanetary (gas-rich) disks to main-sequence stars with debris (gas-poor) disks.

TWA 7 has been observed for infrared (IR) excess emission several times. The presence of a disk around TWA 7 was first noted in submillimeter observations by Webb (2000). They measured a flux of 15.5 ± 2.4 mJy at 850 μm. Neither Jayawardhana et al. (1999) nor Weinberger et al. (2004) detected any excess associated with TWA 7 in the mid-IR. However, Low et al. (2005) reported detections of IR excess at 24 and 70 μm toward TWA 7 with the *Spitzer Space Telescope*. Based on these data and existing shorter wavelength data on the stellar photosphere, Low et al. (2005) derived a disk temperature of 80 K and a lower limit to the mass of 2.4×10^{23} g (3.3×10^{-3} $M_{\rm lunar}$) for the disk. This is a lower limit because the 70 μm data are not sensitive to colder material in the outer disk and dust grains exceeding a few hundred microns in size. A search for substellar companions using the NICMOS (Near-Infrared Camera and Multi-Object Spectrometer) chronograph on the *Hubble Space Telescope* did not reveal any evidence of the disk (Lowrance et al. 2005); a nearby point source is identified as a background object.

The study of debris disks around members of an association permits the study of the evolution of disks as a function of spectral type alone, since the disks likely formed coevally and with similar compositions. It is also possible to judge whether the presence and evolution of disks around multiple stellar systems is comparable to those around single stars. The discovery of disks around low-mass stars is relatively recent (Greaves et al. 1998; Liu et al. 2004; Kalas et al. 2004). The low radiation field of late-K and M dwarfs means that the disks are faint in scattered light compared to disks around more massive stars, and hence they were

TABLE 1
FLUXES OF TWA 7

Wavelength (μm)	Magnitude	Flux (mJy)	Reference
0.44 (*B*)	12.55	39.4	*HST* Guide Star Catalog (Lasker et al. 1996)
0.44 (*B*)	12.3	49.7	USNO-A2.0 (Monet et al. 1998)
0.54 (*V*)	11.06	142.4	Reported in Low et al. (2005)
0.64 (*R*)	11.2	97.4	USNO-A2.0 (Monet et al. 1998)
1.25 (*J*)	7.78	1259.5	Webb et al. (1999)
1.65 (*H*)	7.13	1476.3	Webb et al. (1999)
2.16 (*Ks*)	6.90	1159.1	2MASS PSC
2.18 (*K*)	6.89	1148.8	Webb et al. (1999)
12	...	70.4 $\pm$ 8.6	Weinberger et al. (2004)
24	...	30.2 $\pm$ 3.0	Low et al. (2005)
70	...	85 $\pm$ 17	Low et al. (2005)
450	...	23 $\pm$ 7.2	This work
850	...	9.7 $\pm$ 1.6	This work

NOTES.—Conversion from magnitudes to janskys has been done using zero points from *Allen's Astrophysical Quantities* (Cox 2000). The 12 μm estimate by Weinberger et al. (2004) agrees with that of Jayawardhana et al. (1999) to within 1 σ and is consistent with the photospheric flux expected from TWA 7.

less frequently targeted by scattered-light searches for disks. However, scattered-light imaging is often a follow-up technique used after an IR excess has been discovered (e.g., AU Mic; Kalas et al. 2004). In fact, the low radiation fields may favor long-lived and slowly evolving disks, since some disk material may be unchanged from the original protoplanetary disks (e.g., Graham et al. 2007). *Spitzer* has detected evidence of disks around a few K stars (Chen et al. 2005; Bryden et al. 2006; Uzpen et al. 2005; Gorlova et al. 2004; Beichman et al. 2005), but Beichman et al. (2006) note that in a sample of 61 K1–M6 stars, no excess emission is detected at 70 μm. This is well below the expected detection rate if the disk fraction is at all comparable to the $\sim$15% observed around solar-type stars. The discovery of disks around K- and M-type dwarfs may be difficult at far-IR wavelengths because material at similar radii to disks around early-type stars will be cool and will not radiate sufficiently. However, submillimeter observing sensitivities and the dust temperature conspire to allow these objects to be discovered at submillimeter wavelengths (Zuckerman 2001). Submillimeter observations are sensitive to colder, larger grains, which are more likely to be optically thin than the warmer far-IR emitting dust (Hildebrand 1983).

We report here detections of submillimeter excess emission at 450 and 850 μm around TWA 7 using the James Clerk Maxwell Telescope (JCMT). In § 2 we summarize our observations. In § 3 we present our results. We discuss the relevance of these data to the TWA and the population of disks around low-mass stars in § 4; our results are summarized in § 5.

2. OBSERVATIONS AND DATA REDUCTION

Observations were made in 2004 October 19 using the photometry mode on the Submillimeter Common User Bolometer Array (SCUBA) on the JCMT (Holland et al. 1999). The pointing center of the observation was $\alpha = 10^{\rm h}42^{\rm m}30.3^{\rm s}$, $\delta = -33^\circ40'16.9''$ (J2000.0). The on-source integration time was 1.6 hr. Flux calibration was done using Mars, yielding flux conversion factors (FCFs) of 289.2 $\pm$ 1.4 Jy beam^{-1} V^{-1} at 850 μm and 367.5 $\pm$ 15 Jy beam^{-1} V^{-1} at 450 μm. The absolute flux calibration is accurate to $\sim$20%–30%. Pointing was checked on the source 1034−293. The weather was excellent during the observations, with a τ(225 GHz) value of $\sim$0.04, as measured by the Caltech Submillimeter Observatory. The extinction was corrected using skydips to measure the tau at 850 and 450 μm. The mean tau value was 0.15 at 850 μm in four skydips and 0.59 at 450 μm in three skydips. The extinction values derived from the skydips were consistent with the values extrapolated from the CSO τ(225 GHz) values according to the relations of Archibald et al. (2002).

The data were reduced using the Starlink SURF package (Jenness & Lightfoot 1998). After flat fielding and extinction correction, we flagged noisy bolometers rigorously; 11 (of 37) bolometers were removed in the long-wavelength array, and 26 (of 91) were removed from the short-wavelength array. The photometry data were then clipped at the 5 σ level to remove extreme values. Short-timescale variations in the sky background were then removed using the mean of all bolometers except the central one in each array. The average and variance were then taken of each individual integration for the central bolometers of the long- and short-wavelength arrays after a clip of 3 σ was applied. In the case of the 450 μm data, the signal-to-noise ratio was improved by applying a subsequent 2 σ clip to the remaining data.

3. RESULTS

We have detected emission toward TWA 7 at both 850 and 450 μm. The fluxes measured are 9.7 $\pm$ 1.6 mJy (6.1 σ) and 23.0 $\pm$ 7.2 mJy (3.2 σ), respectively. Errors are statistical, and do not include the typical flux uncertainty of $\sim$20%–30% for submillimeter single-dish calibration. Using the measured fluxes of the star (Table 1) and recently published *Spitzer* data (Low et al. 2005), we construct the spectral energy distribution (SED) for this source (Fig. 1). The submillimeter data clearly represent an excess of emission over the photospheric emission from TWA 7, as detected at 70 μm by Low et al. (2005).

The flux we measure at 850 μm is only about 70% that measured by Webb (2000). Taking into account the typical 20%–30% uncertainty in absolute flux calibration between epochs, the fluxes become 15 $\pm$ 3.8 mJy (earlier epoch) and 9.7 $\pm$ 2.5 mJy (this work), which are consistent within the errors. The instability of flux calibration in the submillimeter is well known, and may be assuaged somewhat by the ability to flux calibrate more often with SCUBA-2, the next-generation submillimeter camera on the JCMT. In the interests of consistency with the only 450 μm detection (in this work), we adopt the 850 μm flux from the later epoch and do not attempt to combine the two data sets.

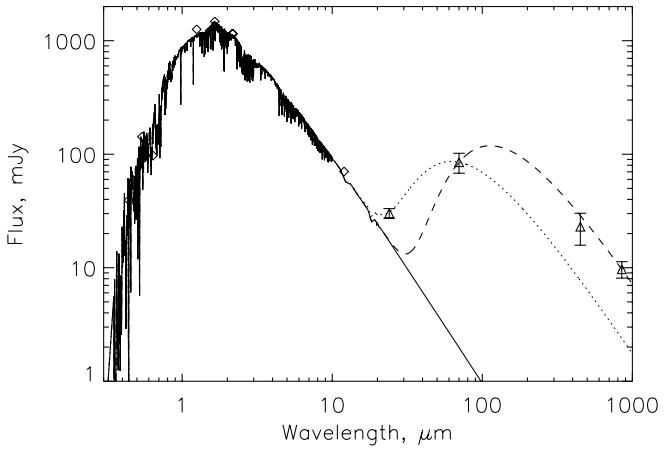

FIG. 1.—SED of TWA 7. The optical and near-IR data (*diamonds*) are modeled with a NextGen model (Hauschildt et al. 1999) scaled to the mass and luminosity of TWA 7 (Low et al. 2005). The star has a temperature of ~3500 K (best fit to stellar photometry; Low et al. 2005; Webb et al. 1999). Triangles mark detections from *Spitzer* and submillimeter detections from the JCMT. These fluxes show clear excess when compared to the stellar photosphere. The flux values are reported in Table 1. Fits for two single-temperature blackbodies (parameters are described in Table 2) to the TWA 7 data show that no single-temperature fits all four measurements of excess emission. An 80 K blackbody, model 1 (*dotted line*), fits the 24 and 70 μm data (Low et al. 2005), but underestimates the submillimeter fluxes. The 70, 450, and 850 μm data are well fit by a 45 K blackbody, model 2 (*dashed line*), but a disk this cold cannot account for the observed 24 μm excess.

3.1. *Submillimeter Excess and Temperature*

Low et al. (2005) derive a disk temperature of 80 K for TWA 7 based on its IR excess values at 24 and 70 μm. The temperature of the star is derived to be 3500 K, which is consistent with the log ($T_{\rm eff}$) of 3.56 reported by Neuhäuser et al. (2000) based on the stellar SED.

Figure 1 shows the flux density distribution toward TWA 7. The stellar fluxes and fit to the stellar photosphere are taken from Low et al. (2005) based on NextGen models by Hauschildt et al. (1999) using a grid of Kurucz (1979). The submillimeter excesses are evident when compared with the stellar spectra. Based on their detection of TWA 7 in the mid-IR, Low et al. (2005) determine that the dust orbiting TWA 7 exists at radii $\geq$7 AU from the star and has a temperature of 80 K. We have constructed several models for dust emission around a 0.55 $M_\odot$ star (see Table 2 for their parameters). We present two single-temperature models in Figure 1, neither of which is capable of fitting the measured excess fluxes at all four wavelengths. Model 1 (dotted line in Fig. 1) is that of Low et al. (2005): a blackbody of 80 K, which fits the 24 and 70 μm data, but cannot reproduce the fluxes at longer wavelengths. Model 2 is a colder blackbody at a temperature of 45 K (dashed line of Fig. 1), which fits the three longest wavelength fluxes, but cannot reproduce the 24 μm flux. Thus, we conclude that the dust in this disk cannot be at a single temperature; rather there are a range of temperatures responsible for the observed emission.

Two models that are able to fit the observed emission spectrum are shown in Figure 2. In both models the dust has a range of temperatures; however, there are two different physical motivations behind the origin of this range.

In model 3 (dotted line of Fig. 2), the dust is assumed to all lie at the same distance from the star, r_0. It is assumed to have a range of sizes with a power-law distribution defined by the relation $n(D) \propto D^{(2-3q)}$ for grains of size D. This power law is assumed to be truncated below dust of size $D_{\rm min} = 0.9$ μm, the size for which $\beta = F_{\rm rad}/F_{\rm gra} = 0.5$ for compact grains. The dust is composed of compact spherical grains of a mixture of organic refractories and silicates (Li & Greenberg 1997), and interaction with stellar radiation determines the temperature that dust of different sizes attains. The same model was used in Wyatt & Dent (2002) to model the emission from the Fomalhaut disk, where more detail can be found on the modeling method. The emission spectrum could be fitted by dust at a radius $r_0 = 100$ AU with a size distribution described by $q = 1.78$. The temperatures of dust in this model range from 21 K for the largest grains (>100 μm) to 65 K for the smallest grains (0.9 μm).

The size distribution used in model 3 is close to that expected in a collisional cascade wherein dust is replenished by collisions between larger grains, since this results in a size distribution with $q \sim 1.83$ and would be truncated below the size of dust for which radiation pressure would place the dust on hyperbolic orbits as soon as they are created. The effect of radiation forces on small grains is quantified by the parameter $\beta = F_{\rm rad}/F_{\rm gra}$ (which is not to be confused with the index of dust emissivity of grains that moderates the Rayleigh-Jeans tail of the SED of cold dust), and it is dust with $\beta > 0.5$ that is unbound. However, due to the low luminosity of M stars, it is not clear whether radiation pressure is sufficient to remove dust grains from the disk system. Figure 3 shows β as a function of dust grain size for dust around TWA 7 ($M_* = 0.55$ $M_\odot$, $L_* = 0.31$ $L_\odot$). While β is larger than 0.5 for compact (<0.9 μm) grains, this condition is only met for a narrow region of the size distribution. Furthermore, if the dust grains are porous, as around AU Mic (Graham et al. 2007), then no grains will have $\beta > 0.5$. An alternative origin for the small grain cutoff could be stellar wind forces, since these provide a pressure force similar to radiation pressure (Augereau & Beust 2006), and it is known that stellar wind forces can be significantly stronger than radiation forces for M stars (Plavchan et al. 2005). While the smallest grain size in the distribution may differ from our value of 0.9 μm, this does not affect the ability of the model to fit the observed emission spectrum with suitable modifications to the slope in the size distribution and radius of the dust belt.

In model 4 (dashed line of Fig. 2), the dust grains are assumed to lie at a range of distances from the star, but they are all assumed to emit like blackbodies, and so have temperatures $T = 278.3$ $L_*^{0.25}/\sqrt{r}$. The spatial distribution of the grains was taken from the model of Wyatt (2005) in which dust is created in a planetesimal belt at r_0, and then migrates inward due to Poynting-Robertson (P-R) drag, but with some fraction of the grains removed by mutual collisions

TABLE 2
DUST MODEL PARAMETERS

Model	Figure Plot	Temperature (K)	$D_{\rm min}$ (μm)	$D_{\rm max}$ (m)	q	Radius (AU)	Mass ($M_\oplus$)
1.....	*Dotted*, Fig. 1	80	...	...	...	...	0.025
2.....	*Dashed*, Fig. 1	45	...	...	...	...	0.2
3.....	*Dotted*, Fig. 2	21–65	0.9	1	1.78	100	6.0
4.....	*Dashed*, Fig. 2	>38	...	...	...	$\leq$35	0.2

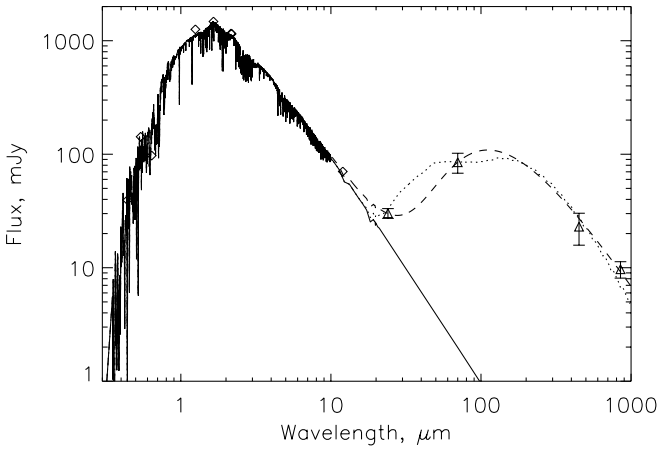

FIG. 2.—Measured SED for TWA 7. Symbols and fit to the stellar spectrum same as in Fig. 1. Two multitemperature models are fit to the excess emission arising from the disk. These are described in detail in the text, and the parameters are summarized in Table 2. In model 3 (*dotted line*), different temperatures arise due to grains of different sizes located at a common radius from the star, while model 4 (*dashed line*) contains grains distributed at a range of distances from the star.

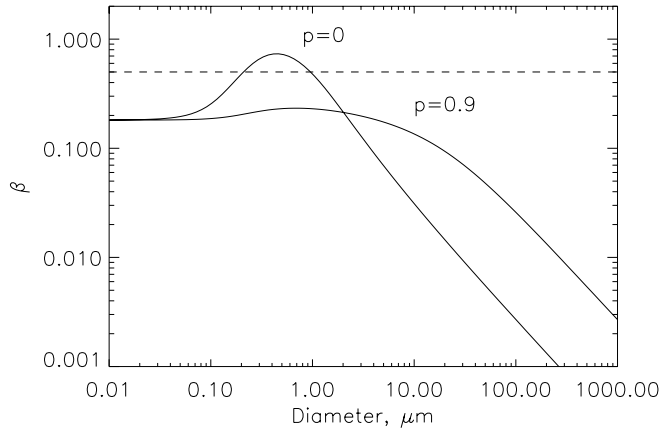

FIG. 3.—Ratio of the radiation force acting on dust grains of different size in the TWA 7 disk to the force of stellar gravity, $\beta = F_{\rm rad}/F_{\rm gra}$. Two different models are shown: compact grains ($p = 0$) and porous grains ($p = 0.9$). Dust with $\beta > 0.5$ is unbound from the star as soon as it is released from a planetesimal. This figure demonstrates that radiation pressure is not a significant mechanism to remove dust grains from the TWA 7 system and is particularly ineffective if the grains are highly porous.

on the way. In the model the dust ends up with a spatial distribution that can be described by the parameter η_0, such that the surface density falls off $\propto 1/\{1 + 4\eta_0[1 - (r/r_0)^{1/2}]\}$. The emission spectrum could be fitted using the parameters $r_0 = 30$ AU and $\eta_0 = 10$, resulting in dust with temperatures upward of 38 K. However, the density of the planetesimal belt required to scale the resulting emission spectrum showed that removal by collisions dominates over the P-R drag force in such a way that η_0 should be closer to 1400 in this disk. Thus, if this model is to have a true physical motivation, then we need to invoke a drag force that is $\sim$140 times stronger than P-R drag. Such a force could come from the stellar wind, which causes a drag force similar to P-R drag and can be incorporated into the model by reducing η_0 by a factor $1 + (dM_{\rm wind}/dt)c^2/L_*$ (Jura 2004). Thus, to achieve $\eta_0 = 10$ in this way we would require the stellar wind to be $\sim$140 times stronger than that of the Sun. The high X-ray luminosity of TWA 7 ($L_{\rm X} = 9.2 \pm 1.0 \times 10^{29}$ ergs s^{-1}; Stelzer & Neuhäuser 2000) may be indicative of a strong stellar wind, since measured mass-loss rates have been found to increase with X-ray flux (Wood et al. 2005). However, the correlation found by Wood et al. (2005; see their Fig. 3) breaks down at X-ray fluxes an order of magnitude lower than that of TWA 7 (for which $F_{\rm X} \sim 8 \times 10^6$ ergs cm^{-2} s^{-1}), and so it is not possible to use this flux to estimate the mass-loss rate with any certainty, and we simply note that the mass-loss rate required to achieve $\eta_0 = 10$ is not incompatible with observations of mass-loss rates of other stars. A stellar wind drag force has also been invoked to explain structure in the AU Mic disk (Strubbe & Chiang 2006; Augereau & Beust 2006).

We note that we are not claiming that the radius, r, size distribution, q, or parameter, η_0, have been well constrained by these fits. The SED does indicate that the disk around TWA 7 contains grains at a range of temperatures. The fits of Figure 2 illustrate two ways in which multiple temperatures in the disk may arise from physically motivated models: the dust could have a range of sizes, or it could be distributed over a range of distances. Other models may also fit the data, including those in which dust has a range of distances and sizes, and those in which the dust originates in not one but multiple dust zones, as has been inferred for AU Mic (M. P. Fitzgerald et al. 2007, in preparation).

The derived fits of Figure 2 do show differences in the mid-IR spectrum. While this suggests that knowledge of the mid-IR spectrum would enable us to distinguish between the two models, it is worth pointing out that the exact shape of this spectrum is very sensitive to the size distributions of small grains (in model 3) and to the radial distribution of grains interior to the planetesimal belt (in model 4). Thus, it is possible that different assumptions about these distributions could be made to provide a fit to the same observed spectrum with both models. The only way to definitively break the degeneracy is through imaging of the thermal emission from the mid-IR to the submillimeter. The single radius disk must look the same at all wavelengths, while a radially distributed disk would look larger at longer wavelengths, as more of the cold dust farther from the star is detected.

3.2. *Mass of the Disk*

Low et al. (2005) estimate the minimum mass in dust of the TWA 7 disk to be 0.0033 $M_{\rm lunar}$, under the assumption that the dust grain size is 2.8 μm. In determining the mass of the disk from submillimeter measurements, a key parameter is the temperature of the dust. Where possible, we discuss the derived mass for each of the models discussed above. For submillimeter fluxes, we can estimate the mass of the disk directly for an assumed temperature and opacity from the relation

$$M_{\rm disk} = \frac{F_\nu\, d^2}{\kappa_\nu\, B_\nu(T_d)}, \qquad (1)$$

where $B_\nu(T_d)$ is the Planck function at the dust temperature, T_d, and κ_ν is the absorption coefficient of the dust. The derived mass is a strongly dependent function of the value of κ_ν. For debris disk studies, a value of 1.7 cm^2 g^{-1} is appropriate at 850 μm (Dent et al. 2000). This is at the upper end of the values derived by Pollack et al. (1994).

We can estimate the mass in model 1 by using the submillimeter flux predicted from the Rayleigh-Jeans tail of the model (2.4 mJy) as well as the 80 K temperature and standard opacity. This gives a mass of 0.025 $M_\oplus$ ($\sim$2 $M_{\rm lunar}$). This can be interpreted as the mass of hot dust, with the proviso that the submillimeter observation shows that there is more mass in colder dust as well.

Model 2 fits the submillimeter and 70 μm emission well. Under the estimate of 45 K for the dust temperature of the disk, the standard dust opacity and the measured 850 μm flux, the TWA 7 disk

contains 0.2 $M_\oplus$ of material (18 $M_{\rm lunar}$). Based on the uncertainty in the flux (random and systematic), the uncertainty on the mass estimates are ~30%. The mass of the TWA 7 disk is an order of magnitude greater than the mass of 0.011 $M_\oplus$ for the disk detected around AU Mic (Liu et al. 2004) that is also derived based on a single-temperature fit to far-IR and submillimeter data with $\kappa_\nu = 1.7$ cm^2 g^{-1}.

Model 3 contains dust grains at different temperatures based on their size. In this case, the size distribution of dust is well defined (i.e., with known scaling); the total mass of dust is given by $M_{\rm tot} = 11 D_{\rm max}^{0.66}$, where $M_{\rm tot}$ is the mass in Earth masses and $D_{\rm max}$ is in meters. While it is impossible to observationally know $D_{\rm max}$ (since large planetesimals are effectively invisible), in our model 95% of the 850 μm flux comes from grains <0.4 m. This implies a mass of 6 $M_\oplus$, significantly higher than that of model 2. In the TWA 7 system, $D_{\rm max}$ could be even larger (or smaller) than this, so this discrepancy carries little definitive weight. The size distribution is relatively shallow (i.e., there are lots of large grains), which explains why the mass is much larger than in model 2.

To derive a mass for model 4 we assume an opacity of 1.7 cm^2 g^{-1} and determine the mass of dust in the model required to reproduce the observed 850 μm flux, given that the dust has a range of temperatures. The derived mass is almost exactly the same as that at of model 2 at 0.2 $M_\oplus$. This is to be expected because the submillimeter flux in both models is dominated by the coldest dust at 38–45 K, and very little additional mass is required in model 4 to explain the mid-IR emission (as illustrated by the low mass in model 1).

Given the inherent assumptions and unknowns in each of these models, we adopt the results of the highly simple model 2 as our most robust estimate of the mass of the dust disk in TWA 7. It depends on the temperature of the grains producing the observed 850 μm flux, which are well fit by the cold dust model of Figure 1. The mass is also highly dependent on the value of κ_ν, for which we have adopted a value in line with other disk modeling work (Dent et al. 2000), and so can be compared with the disk masses derived by other authors (e.g., Wyatt et al. 2003; Liu et al. 2004; Najita & Williams 2005).

4. DISCUSSION

4.1. *Disks in the TW Hydrae Association*

Recent Multiband Imaging Photometer for *Spitzer* (MIPS) data from the *Spitzer Space Telescope* show that most stars in the TWA show no evidence of circumstellar dust out to 70 μm (Low et al. 2005). These results confirm the assertion of Weinberger et al. (2004) and Greaves & Wyatt (2003) that there is a bimodal distribution in the TWA: either stars have strong excesses associated with warm dust emission, or they have very weak emission consistent with very cold disks. The exceptions are the protoplanetary disks around TW Hya and Hen 3-600, which both show evidence of warm and cold disk components (Wilner et al. 2000; Zuckerman 2001).

Lower limits on warm dust emission were set for all TWA members (except TW Hya) by Weinberger et al. (2004). The absence of dust near the star is often taken as a signature of a centrally depleted debris, rather than an accreting, protoplanetary disk. There are a few main-sequence stars for which warm dust is present (i.e., HD 69830 and η Corvi), but this may be a transient phenomenon (Wyatt et al. 2007). Based on their data, Weinberger et al. (2004) deduced that the nondetections implied an absence of material in terrestrial planet regions and that, except for TW Hya, there were no long-lived disks in the association that could still form planets. An outstanding question is whether the stars without warm disks have potential disk material locked up in undetected planets, which would imply that dusty systems represent failed planetary systems, or whether nondetections represent disk systems in which the dust is too cold to be detected in the mid-IR. Only large-scale searches for cold dust around a statistically significant number of stars can clarify whether a sizable population of disks exist that are too cold to detect at mid-IR wavelengths. Such a survey is planned using the new SCUBA-2 camera at the JCMT (Matthews et al. 2007).

The disks now known in the TWA each have very different properties. The disk around TW Hya (K7) still contains molecular gas (Kastner et al. 1997), meaning it is protoplanetary or in a transition from a protoplanetary to a debris disk. It is a broad, face-on disk that extends to 135 AU with evidence of a dip in flux at 85 AU (Krist et al. 2000; Wilner et al. 2000; Trilling et al. 2001; Weinberger et al. 2002; Qi et al. 2004). Hen 3-600 also shows evidence of hosting an accreting, gas-rich disk (Muzerolle et al. 2000). The HR 4796A (TWA 11) disk contains a narrow dust ring at 70 AU from the star (Jayawardhana et al. 1998; Koerner et al. 1998; Schneider et al. 1999; Telesco et al. 2000) and no detectable gas in emission-line studies (Greaves et al. 2000) or more recent searches for absorption due to circumstellar gas along the line of sight (Chen & Kamp 2004), a technique that is highly dependent on the temperature profile of the gas because the disk is not edge-on. In both the Hen 3-600 and HD 98800 systems, the disk orbits only one member of the binary (Jayawardhana et al. 1999; Gehrz et al. 1999) with evidence for cooler dust in circumbinary orbits (Zuckerman 2001). In fact, HD 98800 is a quadruple system, so the dust is in a circumbinary orbit around a spectroscopic binary.

The discussion of the TWA disk population can be illuminated by the results of a recent *Spitzer* study of the Upper Sco Association (with an estimated age of 3–5 Myr) by Carpenter et al. (2006). Their MIPS observation found optically thin disks around A-type stars, no disks around solar-like stars, and optically thick, accreting disks around K- and M-type dwarfs, suggesting that disk evolution proceeds more quickly around higher mass stars. A similar result was found for the H and χ Persei double cluster at 13 Myr (Currie et al. 2007). The sample of stars in Upper Sco was 204 stars with 31 detections at 8 μm, well distributed across spectral types. In the TWA, we have disk detections around only a handful of members, and the association is much smaller, with only 18 members. However, both the optically thick, gas-rich disks in the TWA are hosted by K and M stars, whereas the only A star with a disk hosts an optically thin debris disk. We note that HD 98800 is noted to be gas-poor, but with an optically thick dust disk (Weintraub et al. 2000; Zuckerman & Becklin 1993).

The masses and temperatures of the disks are compared for the TWA members with disks in Table 3. All six disks are detected and their SEDs modeled in the recent paper by Low et al. (2005). Where possible, the masses in Table 3 are derived from submillimeter fluxes or fits to SEDs, rather than IR values that provide lower limits only. This is only an issue for TWA 13, which has not yet been detected at submillimeter or millimeter wavelengths. Scaling $\kappa_{850\ \mu{\rm m}} = 1.7$ cm^2 g^{-1} to 70 μm implies a lower mass limit of 0.1 $M_{\rm lunar}$ based on cold grains.

Of the debris disks, the most massive is the disk around the HD 98800 system, but its mass is comparable to that of the disk around the earlier star HR 4796A. Based on submillimeter masses, the TWA 7 disk is roughly comparable to that of HR 4796A. It is clear that we cannot yet identify a systematic trend in mass or evolutionary phase with spectral type in the TWA. We note that, given the presence of massive disks around components of the multiple

TABLE 3
FLUXES AND MASSES OF DISKS IN THE TWA

Star	Spectral Type	Gas?	Optical Depth	Flux (mJy)	λ (μm)	Mass ($M_{\rm lunar}$)	Temperature (K)	Reference
HR 4796A.....	A0	No	Thin	19.1 ± 3.4	850	19	99	Sheret et al. (2004)
HD 98800	K5	No	Thick	111.1 ± 0.01	800[a]	28	150	Prato et al. (2001)
TW Hya	K7	Yes	Thick	8 ± 1	7000	8×10^5		Wilner et al. (2000) SED fit
TWA 7.....	M1	No	Thin	9.7 ± 1.6	850	18	45	This work
TWA 13.....	M1	No	Thin	27.6 ± 5.9	70	>0.0019	65	Low et al. (2005)
Hen 3-600	M3	Yes	Thick	~65	850	304[b]	20[c]	Zuckerman (2001)

[a] Value of $\kappa_{850\ \mu{\rm m}}$ adjusted by $1/\lambda$.
[b] Mass estimate based on conservative value of $\kappa_{850\ \mu{\rm m}} = 1.7\ {\rm cm}^2\ {\rm g}^{-1}$.
[c] Temperature constraint on cold dust component only.

systems HD 98800 and HR 4796, their dust disk lifetimes do not appear to be any shorter than that around a single star.

4.2. *Disks around Late-type Stars*

Table 4 shows the compilation of the few known debris disks around late-type (K and M) stars. Although a debris disk has been historically claimed around HD 233517 (Skinner et al. 1995), Jura et al. (2006) conclude that it is a giant, not a main-sequence, star, and so we do not include it. Similarly, we exclude HD 23362, although it has a measured excess, because Kalas et al. (2002) attribute the emission to a uniform surrounding dust cloud, not a debris disk, around a K2 III star at 187 pc distance. All fluxes are measured at 850 μm with SCUBA, except where noted. For one of these stars, only an upper limit is observed in the 850 μm flux. Of the eight solid detections, two (HD 92945 and TWA 13) are at a single wavelength in the mid-IR, and two (GJ 182 and GJ 842.2) are detected only in the submillimeter. For the four remaining disks (HD 53143, ϵ Eri, AU Mic, and TWA 7), there is a trend of increasing mass with *later* spectral type, but it must be noted that the mass dependence could also be attributed to the known trend of declining dust masses around older stars (Rhee et al. 2007) in the cases of HD 53143 and ϵ Eri, since they are significantly older than AU Mic and TWA 7. The youngest star, TWA 7, has the most massive disk. We are obviously also biased toward more massive disks at larger distances. AU Mic's disk (9.9 pc) could not have been detected in the observation that detected TWA 7's disk at 55 pc.

Spitzer has made great progress in the last year detecting IR excess from main-sequence stars (see the review by Werner et al. 2006). However, not many of these have been around late-type stars, and for those detections that have been made (Gorlova et al. 2004; Beichman et al. 2005; Uzpen et al. 2005; Bryden et al. 2006; Smith et al. 2006), no estimates of mass in the disk exist. The detections are typically toward field stars or very distant targets in the Galactic plane, although one (P922) is a member of the cluster M47 (Gorlova et al. 2004). We do not list these candidates in Table 4. One exception is the excess around HD 92945 (K1 V), for which Chen et al. (2005) measure a minimum disk mass of $2 \times 10^{-3}\ M_{\rm lunar}$.

As discussed in § 3.1, the degeneracies in the models are best broken with thermal imaging. Of the disks compiled in Table 4, only ϵ Eri (3.3 pc) has been well resolved at submillimeter wavelengths. The distance of the TWA makes imaging of 100 AU (~2″) scale disks impossible with single-dish telescopes in the submillimeter; ϵ Eri would be exceedingly difficult to map if it were even 3 times more distant. We will have to rely on arrays with higher sensitivity to obtain maps like that of ϵ Eri around most low-mass stars unless many more are discovered within 10 pc. In the long-term, mid-IR images will be possible with the planned MIRI (Mid-Infrared Instrument) on the *James Webb Space Telescope*. In the short-term, submillimeter imaging will be possible with the Atacama Large Millimeter-submillimeter Array (ALMA). Far-IR observations will be possible with the *Herschel Space*

TABLE 4
MASSES AND MASS LIMITS OF DEBRIS DISKS AROUND LATE-TYPE MAIN-SEQUENCE STARS

Star	Spectral Type	Distance (pc)	Age (Myr)	Flux (mJy)	λ (μm)	Mass ($M_{\rm lunar}$)	Temperature (K)	Mass Reference
HD 69830[a].....	K0	12.6	600–2000	<7	850	<0.24	100	This work
HD 92945	K1	22	20–150	271	70	>0.002	40	Chen et al. (2005)
HD 53143	K1	18	1000	82.0 ± 1.1	30–34	$>6.5 \times 10^{-6}$	120 ± 60	Chen et al. (2006)
	...	...	...	...	[b]	>0.0096	60[c]	Kalas et al. (2006)
ϵ Eri.....	K2	3	730 ± 200	40 ± 1.5	850	0.1	85	Sheret et al. (2004)
GJ 842.2.....	M0.5	20.9	200	25 ± 4.6	850	28 ± 5	13	Lestrade et al. (2006)
GJ 182[d]	M0.5	26.7	100^{+50}_{-30}	4.8 ± 1.2	850	>2.1	40 + 150[e]	Liu et al. (2004)
AU Mic[d].....	M1	9.9	10	14.4 ± 1.8	850	0.89	40	Liu et al. (2004)
TWA 7[d]	M1	55	8	9.7 ± 1.6	850	18	45	This work
TWA 13[d]	M1	55	8	27.6 ± 5.9	70	>0.0019	65	Low et al. (2005)

[a] We have used the adopted temperature of 100 K, but revised downward the estimated flux and mass based on reanalysis of data originally presented in Sheret et al. (2004). Wyatt et al. (2007) suggest that the warm dust around this source must be transient.
[b] Optical.
[c] Temperature from Zuckerman & Song (2004).
[d] Ages derived from association membership.
[e] Two-component fit.

Observatory, although imaging of 100 AU disks will only be possible for stars within 10 pc.

5. SUMMARY

We have detected submillimeter excess emission arising from the dust disk around TWA 7 at 450 and 850 μm using SCUBA on the JCMT. Based on our photometry and recent data from *Spitzer*, we derive a disk mass of 0.2 $M_\oplus$ (18 $M_{\rm lunar}$) for a temperature of 45 K. This model effectively fits the 70, 450, and 850 μm data with a blackbody. To fit these data and the 24 μm flux requires dust at a range of temperatures, and we show that this could arise from dust at one radius with a range of sizes, or from dust of one size at a range of distances from the star. Based on the SED alone, it is not possible to determine which physical model is dominant.

While the multiple system HD 98800 appears to harbor the most massive debris disk in the TWA, disks of relatively comparable masses are observed around the A0 star HR 4796A and the M1 star TWA 7. Therefore, the formation of debris disks does not appear to be solely a function of the mass of the parent star. A comparison of masses of disks in the TWA reveals no trend in mass or evolutionary state (gas-rich, protoplanetary vs. debris) as a function of spectral type, although the detection of protoplanetary disks around the latest stars is consistent with the results of Carpenter et al. (2006) toward the Upper Sco Association and Currie et al. (2007) in the double cluster H and χ Persei.

Kalas et al. (2006) came to the same conclusion with regard to other debris disks. They surmise that nurture could explain the presence or absence of disks at later epochs. If the environment dynamically heats the disk such that the large planets fail to form, then dust remains for a longer timescale. The dynamically quiet systems then may quickly form planets, leaving no disk to be observed at later epochs, although there is as yet no evidence for any correlation between stars with debris and/or planets (Moro-Martin et al. 2007).

The authors acknowledge our anonymous referee for an insightful and constructive report. As well, the authors thank B. Zuckerman for providing us with the previous 850 μm flux measurement from the thesis of R. Webb, and P. Smith for providing the stellar fit to TWA 7 of Low et al. (2005) to maximize consistency with their analysis. We also acknowledge useful conversations with P. Hauschildt and R. Gray regarding the spectra of M dwarfs. We thank our telescope operator E. Lundin and the staff at the JCMT for their support. B. C. M. acknowledges support of the National Research Council of Canada through a Plaskett Fellowship. P. K. acknowledges support from GO-10228 provided by STScI under NASA contract NAS5-26555. M. C. W. acknowledges support of the Royal Society.

REFERENCES

Archibald, E. N., et al. 2002, MNRAS, 336, 1
Augereau, J.-C., & Beust, H. 2006, A&A, 455, 987
Beichman, C. A., et al. 2005, ApJ, 622, 1160
———. 2006, ApJ, 652, 1674
Bryden, G., et al. 2006, ApJ, 636, 1098
Carpenter, J., et al. 2006, ApJ, 651, L49
Chen, C. H., & Kamp, I. 2004, ApJ, 602, 985
Chen, C. H., et al. 2005, ApJ, 634, 1372
———. 2006, ApJS, 166, 351
Cox, A. 2000, Allen's Astrophysical Quantities (4th ed.; New York: AIP)
Currie, T., et al. 2007, ApJ, 659, 599
Dent, W. R., Walker, H. J., Holland, W. S., & Greaves, J. S. 2000, MNRAS, 314, 702
Gehrz, R., et al. 1999, ApJ, 512, L55
Gorlova, N., et al. 2004, ApJS, 154, 448
Graham, J. R., Kalas, P., & Matthews, B. C. 2007, ApJ, 654, 595
Greaves, J. S., Mannings, V., & Holland, W. S. 2000, Icarus, 143, 155
Greaves, J. S., & Wyatt, M. C. 2003, MNRAS, 345, 1212
Greaves, J. S., et al. 1998, ApJ, 506, L133
Hauschildt, P. H., Allard, F., & Baron, E. 1999, ApJ, 512, 377
Hildebrand, R. 1983, QJRAS, 24, 267
Holland, W. S., et al. 1999, MNRAS, 303, 659
Jayawardhana, R., et al. 1998, ApJ, 503, L79
———. 1999, ApJ, 521, L129
Jenness, T., & Lightfoot, J. F. 1998, in ASP Conf. Ser. 145, Astronomical Data Analysis Software and Systems VII, ed. R. Albrecht, R. N. Hook, & H. A. Bushouse (San Francisco: ASP), 216
Jura, M. 1991, ApJ, 383, L79
———. 2004, ApJ, 603, 729
Jura, M., et al. 2006, ApJ, 637, L45
Kalas, P., Graham, J. R., Clampin, M. C., & Fitzgerald, M. P. 2006, ApJ, 637, L57
Kalas, P., Liu, M., & Matthews, B. 2004, Science, 303, 1990
Kalas, P., et al. 2002, ApJ, 567, 999
Kastner, J. H., Zuckerman, B., Weintraub, D. A., & Forveille, T. 1997, Science, 277, 67
Koerner, D. W., Ressler, M. E., Werner, M. W., & Backman, D. E. 1998, ApJ, 503, L83
Krist, J. E., et al. 2000, ApJ, 538, 793
Kurucz, R. L. 1979, ApJS, 40, 1
Lasker, B. M., Russel, J. N., & Jenkner, H. 1996, The Guide Star Catalog, Version 1.2 (Baltimore: STScI)
Lestrade, X., et al. 2006, A&A, 460, 733
Li, A., & Greenberg, J. M. 1997, A&A, 323, 566
Liu, M., Matthews, B., Williams, J., & Kalas, P. 2004, ApJ, 608, 526
Low, F. J., et al. 2005, ApJ, 631, 1170
Lowrance, P. J., et al. 2005, AJ, 130, 1845
Matthews, B. C., et al. 2007, MNRAS, submitted
Monet, D. G., et al. 1998, The PMM USNO-A1.0 Catalogue (Flagstaff: USNO)
Moro-Martin, A., et al. 2007, ApJ, 658, 1312
Muzerolle, J., Calvet, N., Brinceño, C., Hartmann, L., & Hillenbrand, L. 2000, ApJ, 535, L47
Najita, J., & Williams, J. P. 2005, ApJ, 635, 625
Neuhäuser, et al. 2000, A&A, 354, L9
Plavchan, P., Jura, M., & Lipscy, S. J. 2005, ApJ, 631, 1161
Pollack, J. B., Hollenbach, D., Beckwith, S., Simonelli, D. P., Roush, T., & Fong, W. 1994, ApJ, 421, 615
Prato, L., et al. 2001, ApJ, 549, 590
Qi, C., et al. 2004, ApJ, 616, L11
Rhee, J. H., Song, I., Zuckerman, B., & McElwain, M. 2007, ApJ, 660, 1556
Schneider, G., et al. 1999, ApJ, 513, L127
Sheret, I., Dent, W. R. F., & Wyatt, M. C. 2004, MNRAS, 348, 1282
Skinner, C. J., et al. 1995, ApJ, 444, 861
Smith, P. S., et al. 2006, ApJ, 644, L125
Stauffer, J. R., Hartmann, L. W., & Barrado y Navascues, D. 1995, ApJ, 454, 910
Stelzer, B., & Neuhäuser, R. 2000, A&A, 361, 581
Strubbe, L. E., & Chiang, E. I. 2006, ApJ, 648, 652
Telesco, C. M., et al. 2000, ApJ, 530, 329
Trilling, D. E., et al. 2001, ApJ, 552, L151
Uzpen, B., et al. 2005, ApJ, 629, 512
Webb, R. 2000, Ph.D. thesis, Univ. California, Los Angeles
Webb, R., et al. 1999, ApJ, 512, L63
Weinberger, A. J., Becklin, E. E., Zuckerman, B., & Song, I. 2004, AJ, 127, 2246
Weinberger, A. J., et al. 2002, ApJ, 566, 409
Weintraub, D. A., Kastner, J. H., & Bary, J. S. 2000, ApJ, 541, 767
Werner, M., et al. 2006, ARA&A, 44, 269
Wilner, D., Ho, P., Kastner, J. H., & Rodríguez, L. F. 2000, ApJ, 534, L101
Wood, B. E., et al. 2005, ApJ, 628, L143
Wyatt, M. C. 2005, A&A, 433, 1007
Wyatt, M. C., & Dent, W. R. F. 2002, MNRAS, 334, 589
Wyatt, M. C., Dent, W. R. F., & Greaves, J. S. 2003, MNRAS, 342, 876
Wyatt, M. C., et al. 2007, ApJ, 658, 569
Zuckerman, B. 2001, ARA&A, 39, 549
Zuckerman, B., & Becklin, E. E. 1993, ApJ, 406, L25
Zuckerman, B., & Song, I. 2004, ARA&A, 42, 685